SINTEF Petroleum Research

SINTEF Petroleumsforskning AS
SINTEF Petroleum Research

N-7465 Trondheim, Norway

Telephone: +47 73 59 11 00
Fax: +47 73 59 11 02 (aut.)

Enterprise no.:
NO 936 882 331 MVA

REPORT

TITLE

Characterisation of the Nordland Shale in the Sleipner area by XRD analysis
- A contribution to the Saline Aquifer CO_2 Storage (SACS) project

AUTHOR(S)

Reidar Bøe and Peter Zweigel

CLASSIFICATION	CLIENT(S)
Confidential	SACS-Consortium (BP, ExxonMobil, Norsk Hydro, Statoil, Vattenfall, European Commission, Norwegian Research Council and others)
REPORT NO. 33.0764.00/01/01	

REG. NO.	DATE	PROJECT MANAGER	SIGN.
2001.007	14 February, 2001	Peter Zweigel	*Peter Zweigel*
NO. OF PAGES	NO. OF APPENDICES	LINE MANAGER	SIGN.
23	--	Grethe Schei	*Grethe Schei*

SUMMARY

Sediments of the cap rock sequence above the CO_2-storage unit in the Sleipner area have been studied by qualitative and semi-quantitative XRD analysis of 23 cutting samples from five wells stored at the Norwegian Petroleum Directorate (15/6-5, 15/9-9, 15/9-13, 15/9-14, and 16/7-2).

For well 15/9-9, samples covering the whole thickness of the Pliocene interval have been analysed to characterise vertical variation. Observed vertical mineralogy variations are compared with seismic and well-log patterns.

From all five wells, the interval directly overlying the reservoir units (the Utsira Sand and a sand wedge in the lowermost part of the Nordland Shales) has been analysed, which is expected to provide the primary seal for upward migrating CO_2 both local and regional ('shale drape'). Quartz content of the samples has been related to pore throat radius according to the empirical relationship of Krushin (1997), and the necessary CO_2 column height to cause capillary failure of the seal has been calculated to be approx. 860 m. This is much above expected column heights and capillary failure is thus considered unlikely. Observed migration through shale layers in the Utsira Sand and through a 7 m thick shale package between the Utsira sand and a sand wedge above contrasts to this prediction.

KEYWORDS ENGLISH	KEYWORDS NORWEGIAN
XRD analysis	XRD-analyse
Nordland Shale	Nordlandsleiren
North Sea	Nordsjøen
Sleipner Field	Sleipnerfeltet
CO_2 Storage	Karbondioksydlagring

Table of Contents

1. Background

In the Sleipner area (Norwegian block 15/9; Figure 1-1), CO_2 is injected into the Mio-Pliocene Utsira Sand in which it migrates upwards (e.g. predictions of Baklid et al. 1996 and Lindeberg et al. 2000b and observations in Eiken et al. 2000). The Utsira Sand is overlain by sediments of the Nordland Group (Isaksen & Tonstad 1989; Eidvin et al. 1999), which are reported to be mainly shales in their lower part. These sediments are expected to provide a seal for the Utsira Sands and to inhibit vertical CO_2 migration.

So far, the sediments of the Nordland Group in the Sleipner area have almost exclusively been characterised based on seismic data, wire-line logs and macroscopic description of cuttings (e.g. Lothe & Zweigel 1999). Quantitative description of the fine-grained rocks of this unit, however, requires XRD analysis. Lothe & Zweigel (1999) present analytical results from five samples from the Sleipner area (4 from well 15/9-15 and one from well 15/9-16). Here we document analyses of 23 further cuttings samples from five wells in the same area.

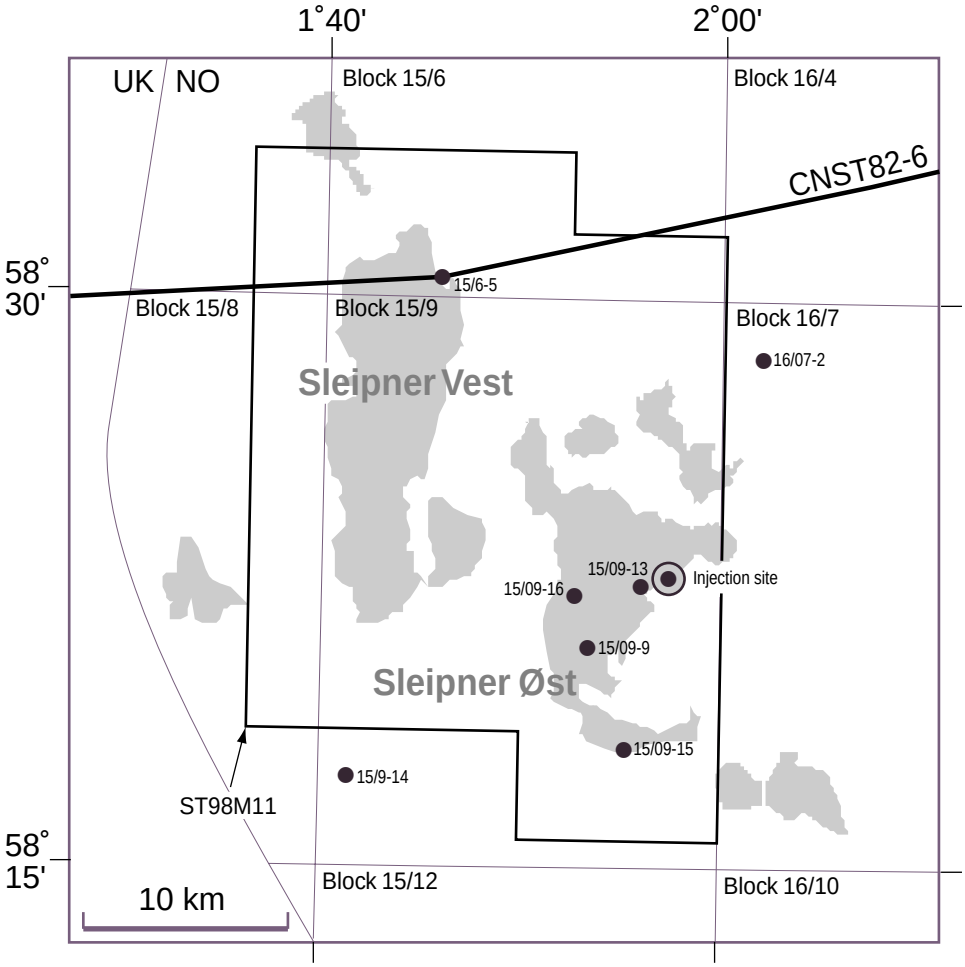

Figure 1-1: Location of sampled wells in the Sleipner area (northern North Sea). The storage site is north-east of well 15/9-13. Wells 15/9-15 and –16 have been sampled previously and are reported in Lothe and Zweigel (1999).

2. Geological Framework and sampling strategy

The lower, upper Pliocene part of the cap rock sequence to the Utsira Sands varies in the Sleipner area between approx. 200 and 300 m thickness (Lothe & Zweigel 1999). It can be divided into three subunits based on seismic (Figure 2-1) and wire-line log patterns (Lothe & Zweigel 1999, Eidvin et al. 1999, Holloway et al. 2000), from top to base:

- An upper Upper Pliocene unit with often high and irregular seismic amplitudes and relatively high density, resistivity, and acoustic velocity as compared to the over- and underlying units; this unit is restricted to the central parts of the basin. Its thickness varies in the Sleipner mainly between 70 to 100 m, but reaches in places up to 129 m.
- A middle Upper Pliocene unit with largely parallel seismic reflectors and gradually downward increasing density, resistivity, and acoustic velocity (with some local deviations from this trend); this unit corresponds to the basinal parts basin-ward prograding sediment wedges, to which it can be correlated on regional seismic lines (Figure 2-1). This unit is about 100 to 150 m thick in the Sleipner area.
- A lower Upper Pliocene unit ('shale drape') directly overlying the Utsira Sand, characterised by parallel reflections both in the basin centre (Sleipner area) and towards the basin margin; the prograding wedges of the middle unit downlap onto the top of his lower unit. We were not able to identify a clear criterion to distinguish the shale drape from the overlying middle unit in wire-line logs. The lower unit contains in the Sleipner area an eastward thickening sand wedge of 0 to approx. 25 m thickness (Zweigel et al. 2000b). The shales of this unit above the sand wedge or – where the sand wedge is absent – above the top Utsira Sand are aprox. 50 m thick.

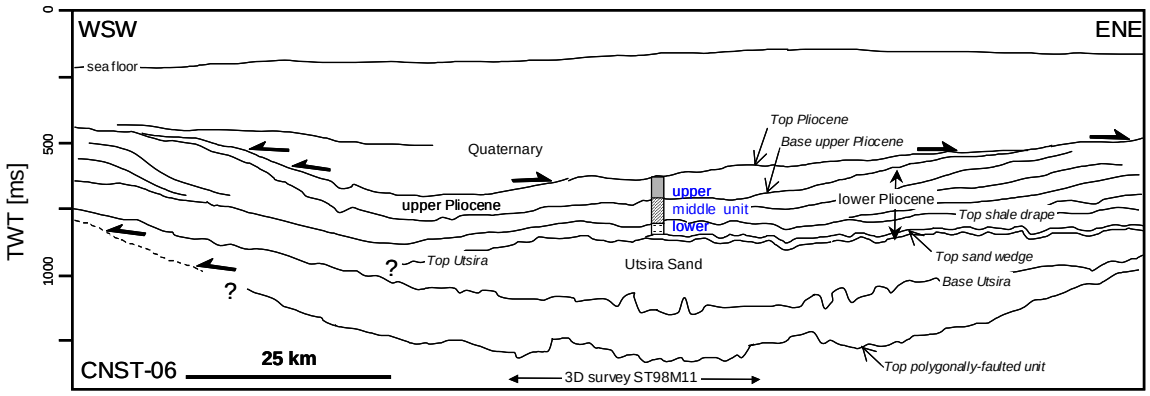

Figure 2-1: W-E section through the Sleipner area and its surroundings based on seismic line CNST82-06 (after Zweigel et al. 2000b).

The shale drape will act as the first seal above both the Utsira Sand proper and the sand wedge. In the Sleipner area it is overlain by the basinal equivalents to the prograding wedges, which are expected from wire-line log data and from depositional models to be fine-grained, and to provide accordingly an additional seal. Closer to the basin margins, this middle unit may contain sand or silt stringers (Chadwick et al. 2000b) which may act as migration pathways. The shale drape, however, might there inhibit upward

migration. Its sealing capacity is therefore both of local and of regional importance. Our sampling had consequently a strong focus on the shale drape (Table 2-1).

Vertical variation in lithology and mineralogy, as suggested by changes in seismic pattern and log response, has been studied in well 15/9-9, from which a series of samples was sampled that cover the range from directly above the top sand wedge to the top part of the upper Pliocene unit (Table 2-1).

Several wells were selected from the direct surrounding of the storage site, to get data characterising the cap rock there (Figure 1-1). Well 15/9-13, which is the well closest to the injection site was our prime candidate for a study of the vertical variations in the Pliocene. Scarcity of samples prohibited this choice. Wells 15/6-5 and 16/7-2 were sampled because they are positioned in the directions of potential migration below the top Utsira sand or within the sand wedge, respectively (Zweigel et al. 2000a). Well 15/9-14 was chosen to provide more regional cover.

The choice of wells and of precise sample depths depended on availability, quantity, and quality of cuttings samples at the Norwegian Petroleum Directorate's core store.

Table 2-1: Position of studied wells and depths (in m TVDss) of stratigraphical and lithological boundaries and of samples. Wells 15/9-15 and –16 were analysed previously and results are documented in Lothe & Zweigel (1999). n.p.: no sand wedge present in that well.

Well	**15/6-5**	**15/9-9**	**15/9-13**	**15/9-14**	**15/9-15**	**15/9-16**	**16/7-2**
UTM North	6486108	6467988	6470978	6461868	6462991	6470539	6482040
UTM East	427977	435038	437652	423259	436816	434402	443667
Top Utsira	789	830.5	844	901	867	818	798
Top sand wedge	n.p.	819	822	n.p.	858.5	n.p.	769
Base upper Plioc.unit		660			700		
Top Pliocene		591			632		
Samples	740	575	795	835	580	800	715
	760	595	805	855	630		735
		615			650		
		635			790		
		655			800		
		775					
		695					
		715					
		735					
		755					
		775					
		785					
		795					
		805					
		815					

3. X-ray diffraction analysis

3.1 Sample examination and preparation

Dry cuttings, mainly washed, but also unwashed samples, had been collected in plastic bags from the core store of the Norwegian Petroleum Directorate in Stavanger. The samples were examined under a Wild M420 photomacroscope, and cuttings for XRD analysis were plucked with small pincers. Images were obtained from selected samples by means of a SONY CCD-IRIS colour video camera and Snappy frame grabber. They both show complete cutting samples and samples purified by plucking (Figures 2-1 to 2-25). Foreign fragments of gneiss and crystalline rock were avoided.

Depths are given below in total vertical depth below sea level (TVDss). The transformation between measured depth along the drill path (MD), which is the depth information at the core store, and TVDss was done by subtracting 25 m. Actual differences between TVDss and MD are given in Table 3-1.

*Table 3-1: Difference (RBK) between measured depth along the drill path (MD) and total vertical depth below sea level (TVDss) for the studied wells. *: not analysed here, XRD analyses presented in Lothe & Zweigel (1999).*

Well	RBK (m)	Well	RBK (m)
15/6-5	24	15/9-15 *	25
15/9-9	25	15/9-16 *	25
15/9-13	25	16/7-2	25
15/9-14	25		

From well 15/9-14, 855 m (Fig. 3-17 and 3-18), both grey (Fig. 3-19) and red shale (Fig. 3-20) were plucked for analysis. Abundant sand grains present in this and the neighbouring sample (860 m) (Fig. 3-18 and 3-21) suggests that the drill bit has penetrated a sandstone horizon in this interval. Also from 15/9-9, 635 m (Fig. 3-7), two samples were plucked for analysis: a grey shale (Fig. 3-8) and cuttings looking like a very fine-grained sandstone, or silt (Fig. 3-9 and 3-10). The identity of the latter is uncertain, and it may represent lumps of compressed rock powder formed at the drill bit, or even concrete.

A few samples with not sufficient washed cuttings had to be washed and dried at 40 °C over night. Sample 15/9-9, 575 m (Fig. 3-15), almost entirely disaggregated when washed, and only a few lumpy aggregates were left (Fig. 3-16).

The dry, plucked samples were ground in an agate mortar until all solid particles were in the silt fraction or finer, and mounted as unoriented powder in sample holders. In a normal sample holder about 1 - 1.5 grams of powder is needed. Two samples (15/9-13, 795 m, and 15/9-14, 855 m, red shale) did not have sufficient material for analysis with such holder, and it was necessary to apply glass discs made to fit into the sample holder. In the centre of the discs a cylindrical hole, 1 millimetre deep, had been drilled out. Different hole diameters were used: 6, 8 and 10 millimetres, allowing samples as small as 0.06 grams to be analysed. The dry powder

was mounted in the holes in the glass discs, and in this case samples of 0.14 and 0.17 grams were analysed with discs having the largest hole diameter.

OVERVIEW PHOTOMICROGRAPHS

Well 15/6-5

Figure 3-1 Cutting sample from well 15/6-5, 635-645 m. Abundant sand may indicate sandstone in the drilled interval. A 2 mm scale bar is shown.

Figure 3-2 Cutting sample from well 15/6-5, 635-645 m. A 2 mm scale bar is shown.

Figure 3-3 Selected shale fragments for XRD analysis from well 15/6-5, 635-645 m. A 2 mm scale bar is shown.

Well 15/9-9

Figure 3-4 Cutting sample from well 15/9-9, 815 m. A 2 mm scale bar is shown.

Figure 3-5 Cutting sample from well 15/9-9, 815 m. A 2 mm scale bar is shown.

Figure 3-6 Selected shale fragments for XRD analysis from well 15/9-9, 815 m. A 2 mm scale bar is shown.

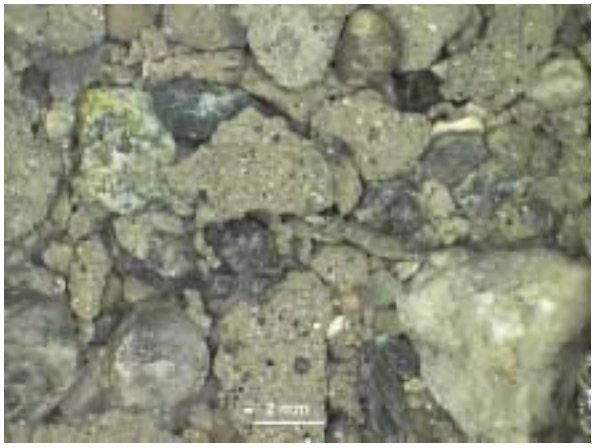

Figure 3-7 Cutting sample from well 15/9-9, 635 m. Grey shale had already been picked out when the image was exposed. A 2 mm scale bar is shown.

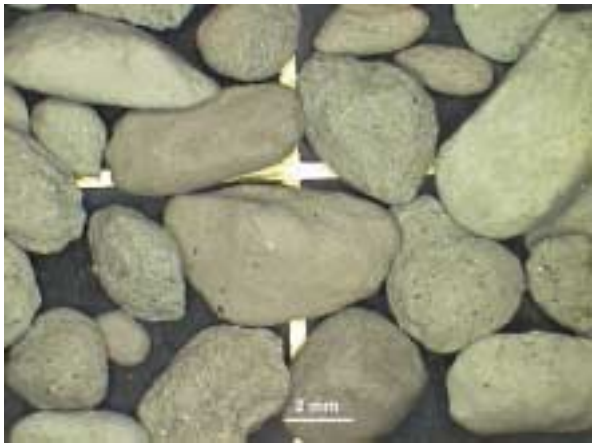

Figure 3-8 Selected grey shale fragments for XRD analysis from well 15/9-9, 635 m. A 2 mm scale bar is shown.

Figure 3-9 Selected fragments from well 15/9-9, 635 m. Their identity is uncertain: dry crust of sand and mud, sandstone, or concrete. A 2 mm scale bar is shown.

Figure 3-10 Selected fragments for XRD analysis from well 15/9-9, 635 m. A 2 mm scale bar is shown.

Figure 3-11 Cutting sample from well 15/9-9, 615 m. A 2 mm scale bar is shown.

Figure 3-12 Cutting sample from well 15/9-9, 615 m. Grey shale, crystalline rock fragments, and possible sandstone fragment (left). The latter is uncertain, and it may represent concrete or dry crust of drilling mud. A 2 mm scale bar is shown.

Figure 3-13 Cutting sample from well 15/9-9, 615 m. A 2 mm scale bar is shown.

Figure 3-14 Selected shale fragments for XRD analysis from well 15/9-9, 615 m. A 2 mm scale bar is shown.

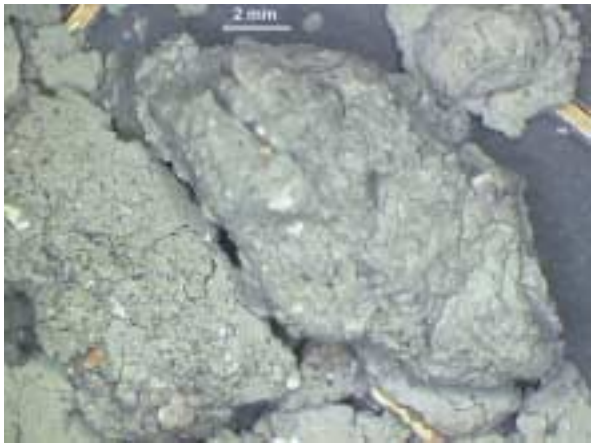

Figure 3-15 Cutting sample from well 15/9-9, 575 m. The unwashed sample almost entirely disaggregated when washed, and only few lumpy aggregates were left. A 2 mm scale bar is shown.

Figure 3-16 Cutting sample from well 15/9-9, 575 m. Dry lumps after attempt to wash the sample. A 2 mm scale bar is shown.

Well 15/9-14

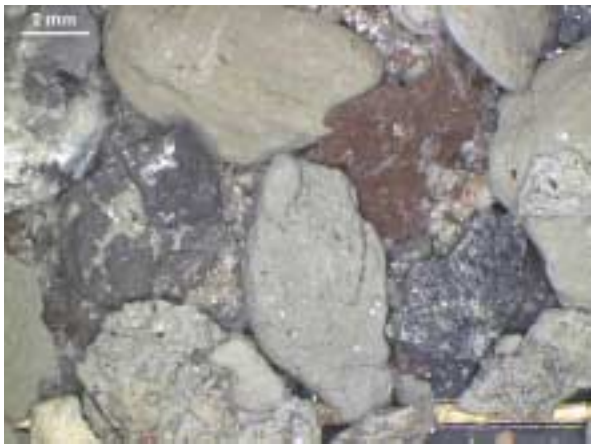

Figure 3-17 Cutting sample from well 15/9-14, 855 m, including grey shale, red shale, crystalline rock fragments and "dry crust". A 2 mm scale bar is shown.

Figure 3-18 Cutting sample from well 15/9-14, 855 m. Grey shale represents the most abundant cuttings, but red shale is also present (<5%). Sand grains may indicate the presence of sand in the drilled interval A 2 mm scale bar is shown.

Figure 3-19 Selected fragments of grey shale for XRD analysis from well 15/9-14, 855 m. A 2 mm scale bar is shown.

Figure 3-20 Selected red shale fragments from well 15/9-14, 855 m. A 2 mm scale bar is shown.

Figure 3-21 Cutting sample from well 15/9-14, 835 m. Red shale fragments occur in addition to grey. Abundant sand grains may reflect presence of sandstone in the drilled interval. A 2 mm scale bar is shown.

Well 15/9-13

Figure 3-22 Cutting sample from well 15/9-13, 805 m. Grey shale, rock fragments, and possible dry crust. A 2 mm scale bar is shown.

Figure 3-23 Cutting sample from well 15/9-13, 805 m. Sand-sized fragments may indicate presence of sandstone horizons. A 2 mm scale bar is shown.

Figure 3-24 Cutting sample from well 15/9-13, 805 m. The dark grey fragments can possibly be sandstone (?). A 2 mm scale bar is shown.

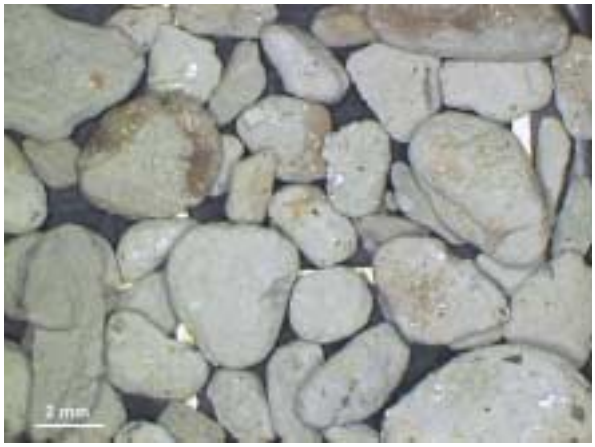

Figure 3-25 Selected grey shale fragments for XRD analysis from well 15/9-13, 805 m. A 2 mm scale bar is shown.

3.2 Methodology

When atomic planes of a mineral in a powder sample attain an appropriate angle, they will diffract the X-rays according to Bragg's Law:

$$n\lambda = 2d \sin \theta$$

where

λ = wave length of the X-rays
d = spacing in the crystal lattice (Å)
θ = angle of diffraction

Each mineral has characteristic reflections on the X-ray diffractogram and can therefore be identified.

The sample preparations were analysed with a Philips PW1710 based X-ray diffractometer with spinner and automatic sample changer at the following conditions:

Range (2θ):	2° - 52°
Radiation:	monochromatic CuK_α
Voltage:	40 kV
Current:	30 mA
Speed:	1°/minute

The mineralogical composition was determined by interpretation of characteristic reflections on the X-ray diffractogram. The quantification of each mineral was based on the product of the peak area (the peak height multiplied with the peak width measured at half the peak height) and a weighed factor (relative to quartz) for the following reflections:

Quartz: (2.28Å + 2.45Å) · 1.0
K-feldspar: 3.24Å · 0.5
Plagioclase: 3.19Å · 0.5
Chlorite: 4.7Å · 2.1 or 7Å · 0.7
Kaolinite: [7Å - (4.7Å · 3)] · 0.7
Mica/Illite: 10Å · 1.0 (mica) or 10Å · 1.4 (illite)
Mixed layer clay minerals (ML): 10 to 14Å · 0.55
Smectite: (14Å - 4.7Å) · 0.35
Calcite: 3.04Å · 0.25
Siderite: 2.79Å · 0.25
Dolomite/ankerite: 2.89Å · 0.2
Pyrite: 2.71Å · 0.7
Hematite: 2.69Å · 0.5
Amphibole: 8.4Å · 0.4
Gypsum: 7.56Å · 0.5
Clinoptilolite: 8.92Å · 0.5

3.3 Results

The interpretation of the XRD-analyses (whole rock) and a semi-quantitative estimation of the crystalline components in the samples are given in Table 3-2. Identification and quantification of minerals occurring in minor amounts (< 2%) are frequently based on a single main reflection, and are therefore uncertain. There is also some uncertainty connected with the numbers calculated for the main minerals (e.g. ± 5% for 50% quartz). It must be emphasized that this method is semi-quantitative, and the use of one decimal in the reported values does not reflect the accuracy of the method. Notice that amorphous material and organic matter is not detected by this method.

Table 3-2 Semi-quantitative mineral composition (weight percentages) of 25 cutting samples from the Sleipner Field.

Well no.	Depth (m)	Qtz	K-fsp	Plag.	Chl.	Kaol.	Mic/Ill	ML	Smect	Calc	Sid	Dol	Pyr	Gyp	Amph	ClO	Hema
15/9-9	575	23.4	2.8	9.2	2.8	14.2	23.7	2.2	2.0	14.0	2.6	0.7	1.5	0.3	0.6	0.0	0.0
15/9-9	595	24.8	3.6	9.9	3.8	14.4	21.8	4.9	2.1	10.0	2.8	0.6	0.7	0.0	0.8	0.0	0.0
15/9-9	615	24.5	3.9	13.6	2.3	15.8	18.8	3.2	2.1	11.6	1.6	0.5	1.5	0.0	0.6	0.0	0.0
15/9-9	*635A	21.5	3.9	20.6	4.4	11.3	22.3	3.3	1.2	7.8	1.5	0.4	0.7	0.0	1.0	0.0	0.0
15/9-9	*635B	29.9	6.9	18.1	4.6	10.8	17.6	2.8	1.2	3.2	1.9	0.5	1.0	0.0	1.5	0.0	0.0
15/9-9	655	15.9	2.8	6.4	2.4	17.0	20.7	8.2	2.3	18.8	2.2	0.6	1.9	0.0	0.3	0.7	0.0
15/9-9	775	19.6	2.5	11.7	3.9	7.5	24.6	7.2	0.9	13.6	2.9	0.4	3.9	0.0	0.9	0.3	0.0
15/9-9	695	20.8	2.7	12.4	5.8	15.3	23.9	2.2	3.8	3.7	4.9	0.7	3.1	0.0	0.8	0.0	0.0
15/9-9	715	18.6	3.0	12.7	5.7	19.9	24.3	1.9	6.0	2.6	1.2	0.6	2.2	0.0	1.2	0.0	0.0
15/9-9	735	22.0	2.6	12.0	4.2	17.7	21.9	1.7	9.5	0.2	2.3	1.0	3.3	0.0	1.1	0.3	0.0
15/9-9	755	18.4	1.9	11.6	5.5	18.8	28.0	1.9	8.9	0.1	1.3	0.6	2.2	0.0	0.9	0.0	0.0
15/9-9	775	21.2	1.8	13.4	3.9	17.5	25.5	1.5	8.2	0.5	1.8	0.8	3.0	0.0	0.9	0.0	0.0
15/9-9	785	20.8	2.0	11.3	5.1	16.4	26.1	0.8	10.6	0.9	1.4	0.7	3.1	0.0	0.6	0.2	0.0
15/9-9	795	19.5	2.0	12.9	2.9	20.4	25.1	1.4	8.5	0.7	1.8	0.7	2.9	0.0	1.1	0.0	0.0
15/9-9	805	24.5	2.5	11.8	4.3	17.6	22.0	1.9	7.9	2.0	1.3	0.8	2.3	0.0	0.8	0.3	0.0
15/9-9	815	20.6	2.6	10.0	3.2	17.8	28.8	1.9	9.1	0.5	1.8	0.6	2.2	0.0	0.9	0.0	0.0
15/6-5	735/745	18.9	4.2	10.6	4.9	14.2	30.0	2.5	9.2	0.9	1.2	0.6	2.0	0.0	0.9	0.0	0.0
15/6-5	755/765	18.4	3.9	12.0	4.0	12.5	36.1	3.0	5.0	0.7	1.5	0.6	1.8	0.0	0.6	0.0	0.0
15/9-13	795	28.5	3.2	12.6	8.0	8.6	19.9	7.9	2.2	0.8	1.9	1.3	4.2	0.0	0.8	0.0	0.0
15/9-13	805	21.6	2.5	9.0	4.5	16.0	29.7	1.8	**9.0	0.5	2.3	0.7	1.9	0.0	0.5	0.0	0.0
15/9-14	835	18.5	2.5	10.1	6.4	19.4	26.8	2.4	8.9	0.0	1.4	0.7	2.0	0.0	0.9	0.0	0.0
15/9-14	Grey 855	20.8	1.6	9.0	6.0	16.4	22.5	0.8	16.2	0.4	0.7	0.8	4.0	0.0	0.8	0.0	0.0
15/9-14	Red 855	29.4	2.3	9.4	19.4	0.0	25.7	0.9	0.2	1.3	0.7	4.8	0.0	0.0	0.0	0.0	6.0
16/7-2	715	22.0	2.1	11.7	2.5	17.9	26.9	2.1	8.2	0.9	0.9	1.0	2.6	0.0	1.0	0.2	0.0
16/7-2	735	20.8	2.0	11.4	5.8	14.5	26.6	1.5	10.6	1.0	1.3	0.8	2.7	0.0	0.8	0.3	0.0

Abbr.: Qtz = quartz, K-fsp = potassium feldspar, Plag = plagioclase feldspar, Chl = chlorite, Kaol = kaolinite, Mic/Ill = mica and illite, ML = mixed layer clay, Smect = smectite, Calc = calcite, Sid = siderite, Dol = dolomite/ankerite, Pyr = pyrite, Gyp = gypsum, Amph = amphibole, ClO = clinoptilolite (zeolite), Hema = hematite.
* = 635A is shale, 635B is uncertain (very fine sand, concrete, compressed rock powder ?).
** = May include some ML-clay.

3.4 X-ray diffractograms

Examples of X-ray diffractograms used for mineral identification and quantification are presented for selected samples.

Figure 3-26 shows the diffractograms of the grey and the red shale from 855 m in well 15/9-14. The red shale is especially richer in quartz, and contains dolomite, hematite (explains the red colour) and chlorite, while the grey shale is rich in smectite and kaolinite, and contains also pyrite.

Figure 3-27 shows the diffractogram of the grey shale at 635 m in well 15/9-9 and also for the cuttings of uncertain identity (looking like very fine sand). The "sand" is richer in quartz and K-feldspar, but contains less mica, plagioclase and calcite. It may possibly represent rock powder compressed to small balls or lumps at the drill bit.

Figure 3-28 shows the X-ray diffractograms for the two samples from 795 and 805 m in well 15/9-13. The diffractograms are very similar, but the elevated red curve of 795 between 14 and 24° 2θ may indicate a higher content of X-ray amorphous material (e.g. organic matter or chert). The smectite peak of 805 is strong and broad and extends almost to the mica peak, while in 795 a broader belt between the mica and smectite peaks is calculated as mixed layer clay. The smectite peak of 805 overlaps with the mixed layer clay to a larger extent, and the calculated amount of smectite may therefore also include some mixed layer clay.

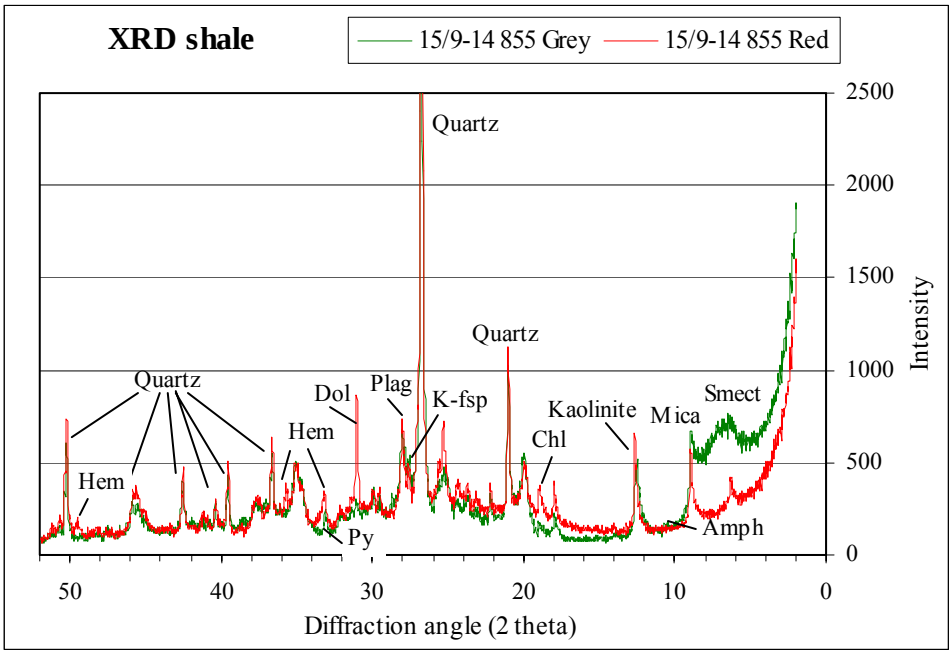

Figure 3-26: The curves represent X-ray diffractograms for the grey (green curve) and the red shale (red curve) from 855 m in well 15/9-14.
Abbreviations: Hem = hematite, Pyr = pyrite, Dol = dolomite/ankerite, Plag = plagioclase, Kfsp = K-feldspar, Chl = chlorite, Mica = mica and illite, Amph = amphibole, Smect = smectite.

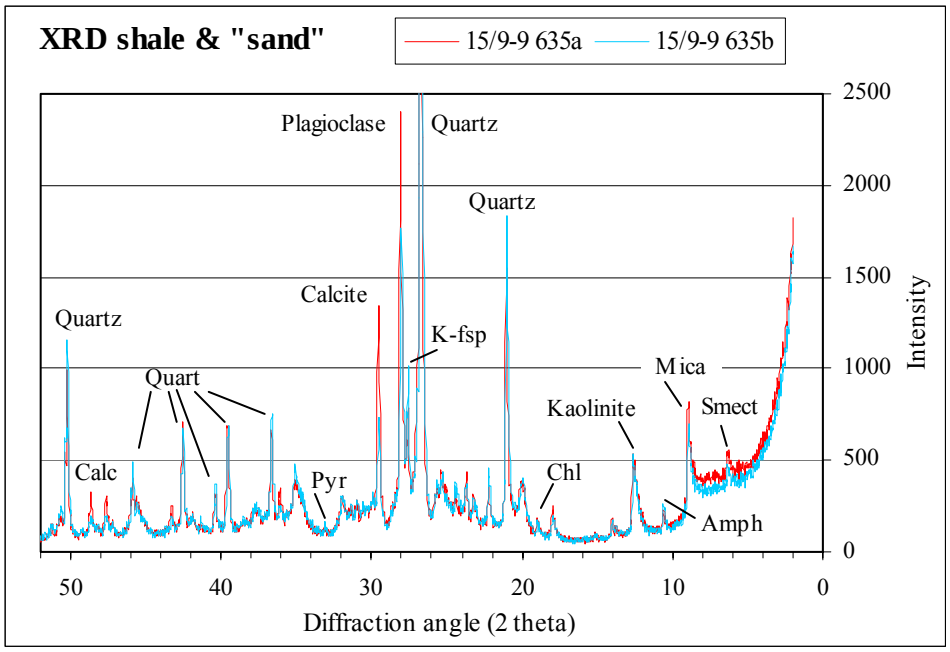

Figure 3-27: X-ray diffractograms of grey shale (red curve) and cuttings looking like very fine sand (blue curve) from 635 m, well 15/9-9.
Abbreviations: Calc = calcite, Pyr = pyrite, Kfsp = K-feldspar, Chl = chlorite, Amph = amphibole, Mica = mica and illite, Smect = smectite.

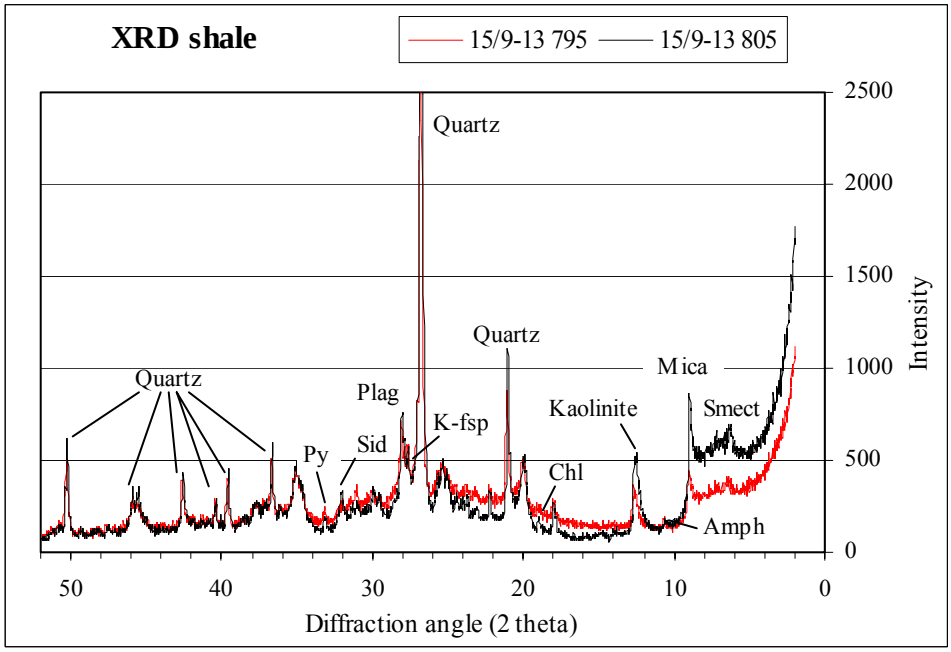

Figure 3-28: X-ray diffractograms for two samples from well 15/9-13, 795 and 805 m.
Abbreviations: Pyr = pyrite, Sid = siderite, Plag = plagioclase, Kfsp = K-feldspar, Chl = chlorite, Amph = amphibole, Mica = mica and illite, Smect = smectite.

3.5 Mineralogy variation with depth in well 15/9-9

Figure 3-29 shows the trend of bulk mineralogy with depth in well 15/9-9. The single points marked at 635 m represent the cuttings looking like very fine sand that occurred together with the grey shale. The quartz content is above 635 m higher than 20 %, and below that depth about 20 %. K-feldspar shows little variation with depth and is consistently low around 10%, but has a peak at 635 m. The smectite content is low (1 – 2 %) down to 675 m, but from there it starts to increase gently up to 8 – 10 %. Kaolinite also gradually increases downwards from this level, up to 18 – 20 %. The content of mica/illite (they overlap in the diffractogram) is consistently high (20 – 30 %), and show a small increase from 735 m.

Mixed layer clay is low, but shows a small peak at 655 – 675 m. Chlorite is generally low, but shows a slightly higher trend between 675 and 795 m. Calcite is most abundant in the upper part (10 – 18 %). From the maximum at 655 m it drops significantly down to 735 m (0.2 %). In the upper part where calcite ($CaCO_3$) is high, siderite ($FeCO_3$) is more abundant than pyrite (FeS_2), while pyrite is higher in the lower part, indicating lower accessibility of CO_3^{2-}. The content of dolomite and amphibole is low.

Figure 3-29 (two rightmost columns) illustrates the variation of the sum of quartz and feldspar (Qtz +Fsp) and the sum of clays and mica (ClayMic) with depth. Apart from the kinks at 635 and 655 m the sum of quartz and feldspar is relatively consistent throughout the whole interval. The kinks are partly due to variations in the plagioclase content, but also a response to the especially high calcite contribution at 655 m. Only in a short interval between 615 and 635 m the Qtz +Fsp curve is higher than the ClayMic curve. The sum of quartz and feldspar is a measure of the silt fraction in shales. The downward increase of the ClayMic curve from 675 m is due to the increase in smectite. This also explains the increase of the Sm/(Q+F) curve (ratio between smectite and the sum of quartz and feldspar). The two curves Sm/Clay (the ratio between smectite and the sum of clays and mica) and Sm/(Cl-Sm) (the ratio between smectite and the sum of clays and mica minus smectite) almost completely overlap, but there exists a split from 675 m and down due to the increased smectite content.

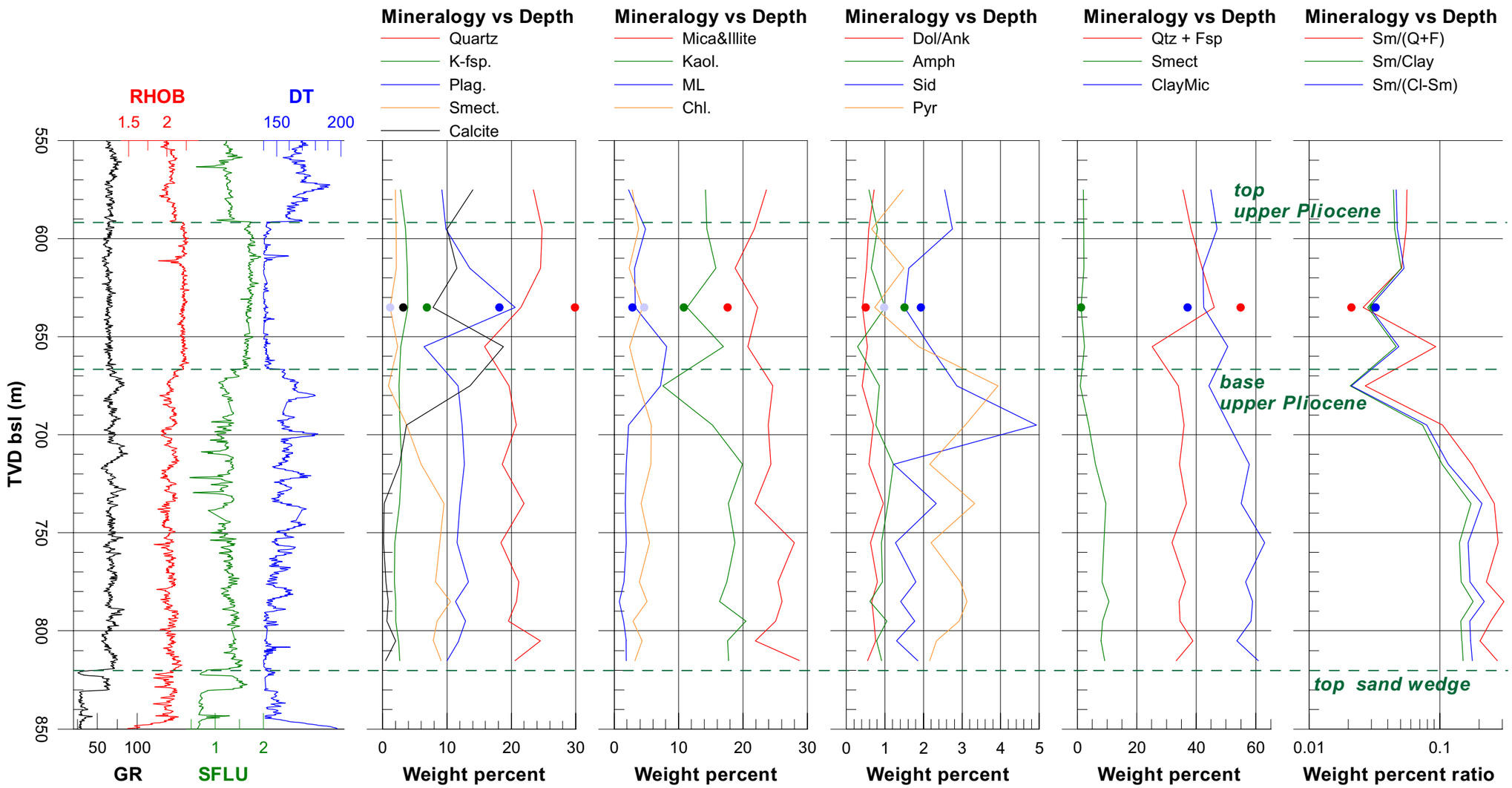

Figure 3-29. Wire-line logs and bulk mineralogy of well 15/9-9 plotted versus depth. The points at 635 m represent the cuttings looking like very fine sand, but may just be compressed rock powder formed at the drill bit. Abbreviations: K-fsp. = K-feldspar, Plag. = plagioclase, Smect = smectite, Mic/Ill = mica and illite, Kaol. = kaolinite, ML = mixed layer clay, Chl. = chlorite, Sid = siderite, Pyr = pyrite, Amph = amphibole, Calc = calcite, Dol = dolomite and ankerite. Qtz+Fsp = sum of quartz and feldspar, ClayMic = sum of clays and mica, Smect = smectite, Sm/(Q+F) = ratio of smectite and the sum of quartz and feldspar, Sm/Cl = ratio between smectite and sum of clays, Sm/(Cl-Sm) = the ratio between smectite and clay not including smectite.

Relation to seismic and log-defined units

Figure 3-39 allows a comparison of mineralogical trends in well 15/9-9 with wire-line log patterns and in relation to sedimentary units discriminated based on seismics. Lithology is nearly constant within the lower unit (shale drape), being in accordance with the seismic pattern, which suggests basin-wide uniform sedimentation during deposition of the shale drape.

The middle unit is in terms of lithology a transition zone between the lower and upper units. It has upward increasing calcite and mixed layer clay mineral content and upward decreasing smectite and total clay content (the latter largely due to the calcite increase). The significance of the siderite peak at 695 m is not clear, this may be a local effect. The observed gradual changes within this unit may be related to the approach of the sediment wedges at the basin margins, to which this unit is the basinal equivalent. Note that this unit on wire-line logs does not have a transitional character between lower and upper Upper Pliocene units.

The upper unit, which has on seismics and wire-line logs a clearly different signature than the lower and middle unit, is characterised by a relatively high calcite and mixed layer clay mineral content. The smectite content is relatively low as is the total clay mineral and mica content. Quartz shows an upward increase within the upper unit. The lithology transition from the middle to the upper unit is gradual and there is no significant lithology change at its top. This is in contrast to the clearly visible, abrupt changes on most wire-line logs (note however the constancy of the gamma-ray log) and to the strongly different depositional geometries visible on seismics.

Our analyses concentrated on selected, relatively large shale pieces from the cuttings samples. As evident from Figures 3-1 to 3-25, many of the cuttings samples prior to picking contained a considerable fraction of sand-size grains. Their origin is uncertain, but they may have been derived from the analysed interval itself. As a general tendency, samples from the upper unit contained relatively more sand grains than those from below. It is difficult to assess if this is due to a higher quartz content of the upper unit or due to a stronger mixture with sand-rich material from the Quaternary.

Macroscopic inspection of the samples showed that the interval from 615 to 675 contained relatively many large clasts (up to 5 mm in diameter) of crystalline material (gneiss, black siliceous clasts). This accords with the general observation of Eidvin et al. (1999) who reported large proportions of pebbles of crystalline and sedimentary origin for the whole Upper Pliocene interval. They interpreted them to indicate a glaciomarine depositional environment.

The occurrence and abundance of smectite may reflect climatic conditions. Its reduced abundance in the upper half of the Pliocene interval may accordingly be due to climatic cooling.

3.6 Mineralogy of the lower part of the shale

The lower part of the Pliocene shale package was sampled and analysed in all wells reported here and in the two wells reported in Lothe & Zweigel (1999). Note, however, that the samples have a distance of up to several 10s of metres above the top Utsira Sand or the top sand wedge (Table 3-3). Unavailability or scarcity of cuttings material prevented sampling and analysis of samples closer to the top sand in several wells.

Table 3-3 Calculated mineralogical parameters from semi-quantitative mineral analysis (weight percentages) of cutting samples from the lower part of the Pliocene sequence. Base data are in Table 3-2 and from Lothe & Zweigel (1999).

Well no.	Depth (m)	m above sand	Qtz	Qtz+Fsp	Sm/(Q+F)	ClayMic	Sm/Clay	Sm/(Cl-Sm)
15/9-9	735	75	22.0	36.7	0.260	55.1	0.173	0.209
15/9-9	755	55	18.4	31.8	0.279	63.0	0.141	0.164
15/9-9	775	45	21.2	36.4	0.227	56.6	0.146	0.170
15/9-9	785	35	20.8	34.2	0.309	58.9	0.179	0.219
15/9-9	795	25	19.5	34.5	0.245	58.4	0.145	0.169
15/9-9	805	15	24.5	38.8	0.203	53.7	0.147	0.172
15/9-9	815	5	20.6	33.3	0.274	60.7	0.15	0.176
15/6-5	735/745	50	18.9	33.7	0.273	60.8	0.151	0.178
15/6-5	755/765	30	18.4	34.3	0.146	60.5	0.083	0.09
15/9-13	795	25	28.5	44.3	0.05	46.6	0.047	0.05
15/9-13	805	15	21.6	33.1	0.272	61.0	0.147	0.172
15/9-14	835	65	18.5	31.2	0.285	63.8	0.139	0.161
15/9-14	Grey 855	45	20.8	31.5	0.515	61.8	0.262	0.355
15/9-14	*Red 855*	*45*	29.4	*41.1*	*0.005*	*46.2*	*0.004*	*0.004*
16/7-2	715	55	22.0	35.9	0.229	57.6	0.143	0.167
16/7-2	735	35	20.8	34.3	0.31	59.0	0.18	0.22
15/9-15	800	60	31.2	48.1	0.048	44.6	0.052	0.054
15/9-16	800	20	21.6	32.9	0.091	66.4	0.045	0.047

Abbreviations: Qtz+Fsp = sum of quartz and feldspar, ClayMic = sum of clays and mica, Smect = smectite, Sm/(Q+F) = ratio of smectite and the sum of quartz and feldspar, Sm/Cl = ratio between smectite and sum of clays, Sm/(Cl-Sm) = the ratio between smectite and clay not including smectite.

The sample 15/9-14 Red 855 is of a special lithology and will not be included in the discussion below. Sample 15/9-13 795 was very small, and the partly extreme analytical results may contain a large uncertainty. Selection of rock fragments in the samples reported in Lothe & Zweigel (1999) was not restricted to large shale components as in the present study, but included parts of the smaller grains. This is a reason for the often higher quartz contents

in these samples, as especially in sample 15/9-15 800. Results from the samples listed in this paragraph are therefore treated with lower importance than the others.

The quartz content in the analysed samples of this unit varies between 18.4 and 35.8 wt%, but most samples have a quartz content of around 20 wt% and below 25 wt% (Table 3-2 and Lothe & Zweigel 1999). Variations in the quartz content dominate variations in Qtz + Fsp, which range from 31.2 to 39 wt% (41.1 and 48.1 wt% in unsure samples). Total clay and mica contents are mainly in the range 54 – 66 wt%, with some exceptions in previous samples (down to 40.5 wt%) and in the small sample 15/9-13 795.

Seal capacity estimated from quartz content

Krushin (1997) describes a methodology that relates the mineralogy of non-organic shales (especially their quartz content) to the displacement pore throat size, which defines the seal capacity of a shale. His results show that the higher the quartz content of a shale, the larger is the pore throat size and the lower is the seal capacity (he does not clearly define the pore throat size, but we anticipate that it is the pore throat diameter). In our case, the range of displacement pore throat radii would then predominantly be between approx. 4 to 7.5 nm (for quartz contents between 20 and 25 weight-%), and up to approx. 15 nm (for a quartz content of 36 weight-%).

Given the surface tension between water and CO_2 σ, the displacement pore throat radius r can be related to the capillary entry pressure. Following the conservative simplifications of Lindeberg (1997), the required pressure difference Δp for CO_2 to enter a water wet shale pore (or throat) can be calculated as

$$\Delta p = 2\,\sigma / r$$

Lindeberg (1997) states a typical surface tension value of 35 mN/m, but close to the critical point of CO_2, as it is the case in the Sleipner injection case, surface tension may be as low as 20 mN/m (Lindeberg, pers. comm. 2001). Application to the maximum value for the displacement pore throat size determined in the present study (15 nm), the capillary entry pressure can be calculated to be 2.6 MPa. This is a conservative value, because a low value for σ and a high value for r have been used. If Krushin (1997) meant pore throat radius with his 'pore throat size', the capillary entry pressure would be 1.3 MPa.

With a density difference between CO_2 and water at reservoir conditions of approx. 300 kg/m^3 (Lindeberg et al. 2000a), a 1 m thick CO_2 column will create a pressure difference of 0.003 MPa. Accordingly, a more than 860 m high CO_2 column would be required to cause capillary top seal failure at a capillary entry pressure of 2.6 MPa. The Utsira Sand itself has in the Sleipner area a maximum thickness of about 300 m, and simulated equilibrium column heights in structural traps in the area reach 26 m at maximum (Zweigel et al. 2000a&b). Capillary leakage of CO_2 through the top seal is therefore unlikely to occur.

This result is in contrast to the observed migration of CO_2 through several, about 1 m thick shale layers within the Utsira Sand and through the approx. 7 m thick shale layer

between the Utsira Sand proper and the westward thinning sand wedge in the lowermost part of the Nordland Shale (e.g. Fig. 5.30 in Zweigel et al. 2000b). Limitations for the applicability of the method outlined and used here, and reasons for the discrepancy between predicted seal tightness and observed migration through presumed seal units may be:

- The shales in the Utsira Sand and between sand wedge and Utsira Sand have not been sampled nor analysed, and may have different composition and migration-relevant parameters than the samples analysed in the present study.

- The intra-Utsira shale layers may have partly been eroded during deposition of the overlying sand unit (Lothe & Zweigel 1999). There are, however, no indications for local erosion of the shale below the sand wedge.

- The database of Krushin (1997) is rather limited (the correlation is based on 8 samples, of which 4 have very similar properties). His samples with small pore throats are very rich in calcite or dolomite, while ours are not. Further, the samples used by Krushin (1997) are from rocks of Precambrian to Jurassic age, and it is likely that they are better lithified than the shales analysed here. Better lithification and compaction could increase seal capacity by collapse and/or cementation of pores, but it may as well be decreased by making the shales more prone to contain (micro)-fractures.

- The estimated seal capacities may not be representative for the whole investigated shale unit, but rather for its most clay-rich parts (layers). The washed samples contained grains in the sand-fraction (see Figures 3-1 to 3-25) which we did not include in the XRD analysis. These sand grains may stem from the overlying, reported sand-richer Quaternary interval. They may, however, as well come from thin sandy or silty layers within the lower part of the Upper Pliocene itself. These thin layers would then reduce the average permeability of this interval. Their effect on the effective permeability of the interval is difficult to estimate, because this will depend on the connectivity between the highly permeable layers.

- The prediction argued here regards capillary leakage through the pore network as the only leakage mechanism. In the case of (micro-)fractures being present, these may provide much more effective migration pathways than the pore network.

4. Acknowledgements

Samples were provided by the Norwegian Petroleum Directorate in Stavanger (Frigivingssak 0006) which is greatfully acknowledged.

5. References

Baklid, A.; Korbøl, R.; & Owren, G. 1996: Sleipner Vest CO2 disposal, CO2 injection into a shallow underground aquifer. Paper presented on the 1996 SPE Annual technical Conference and Exhibition, Denver, Colorado, USA, SPE paper 36600, 1-9.

Chadwick et al., (2000): Saline Aquifer CO2 Storage (SACS2) – Progress report 01/0700 – 31/12/00. British Geological Survey, 22 pp.

Eidvin, T., Riis, F., & Rundberg, Y., 1999: Upper Cainozoic stratigraphy in the central North Sea (Ekofisk and Sleipner fields). *Norsk Geologisk Tidsskrift*, 79, 97-128.

Eiken, O., Brevik, I., Arts. R., Lindeberg, E., & Fagervik, K. 2000: Seismic monitoring of CO_2 injected into a marine aquifer. SEG Calgary 2000 International conference and 70th Annual meeting, Calgary.

Holloway, S. (ed.), 1996: The underground disposal of Carbon Dioxide – Final report. British Geological Survey Report for JOULE II project CT92-0031. 355pp.

Isaksen, D. & Tonstad, K. (eds.), 1989: A revised Cretaceous and Tertiary lithostratigraphic nomenclature for the Norwegian North Sea. *NPD-Bulletin*, 5, 59pp.

Krushin, J.T., 1997: Seal capacity of nonsmectite clays. In: Surdam, R.C. (ed.): Seals, traps, and the petroleum system. AAPG Memoir, 67, 31-47.

Lindeberg, E., 1997: Escape of CO_2 from aquifers. Energy Convers. Mgmt., 38, Suppl., S235-S240.

Lindeberg, E., van der Meer, B., Moen, A., Wessel-Berg, D., & Ghaderi, A., 2000a: Saline Aquifer CO2 Storage (SACS): Task 2: Fluid and core properties and reservoir simulation, Final report. SINTEF Petroleum Research report, 54.5148.00/0200, 42pp., confidential.

Lindeberg, E., Zweigel, P., Bergmo, P., Ghaderi, A., & Lothe, A. 2000b: Prediction of CO_2 dispersal pattern improved by geology and reservoir simulation and verified by time lapse seismic. 5th International Conference on Greenhouse Gas Control Technologies, Cairns (Australia), August 2000.

Lothe, A.E. & Zweigel, P., 1999: Saline Aquifer CO_2 Storage (SACS). Informal annual report 1999 of SINTEF Petroleum Research's results in work area 1 'Reservoir Geology'. SINTEF Petroleum Research report 23.4300.00/03/99, 54 p. Restricted.

Zweigel, P., Hamborg, M., Arts, R., Lothe, A., Sylta, Ø., & Tømmerås, 2000a: Simulation of migration of injected CO2 in the Sleipner case by means of a secondary migration modelling tool – A contribution to the Saline Aquifer CO2 Storage project (SACS). SINTEF Petroleum Research report (CD) 23.4285.00/01/00, 63 p., 6 app., confidential.

Zweigel, P., Lothe, A.E., Arts, R., & Hamborg, M., 2000b: Reservoir geology of the storage units in the Sleipner CO_2-injection case – A contribution to the Saline Aquifer CO_2 Storage (SACS) project. SINTEF Petroleum Research report (CD) 23.4285.00/02/00. 79 pp. & 3 appencices, confidential.